THE ANALYSIS OF UNDEREXPANDED JET FLOWS FOR HYPERSONIC AEROTHERMODYNAMIC APPLICATIONS

Vladimir V. Riabov
Rivier University, Nashua, New Hampshire 03060, USA

Abstract

A method of underexpanded hypersonic viscous jets has been developed to acquire experimental aerodynamic data for wedges, disks, and plates in the transitional regime between free-molecular and continuum regimes. The kinetic, viscous, and rotational nonequilibrium quantum processes in the jets of He, Ar, N_2, and CO_2 under various experimental conditions have been analyzed by asymptotic methods and numerical techniques.

Fundamental laws for the characteristics and similarity parameters are revealed. In the case of hypersonic stabilization, the Reynolds number Re_0 and temperature factor are the main similarity parameters. This research has discovered those conditions, which allow the significant influence of other parameters (specific heat ratio, viscosity parameter, Mach number). The acquired data could be used effectively for research and prediction of aerodynamic characteristics of hypersonic vehicles during their flights under atmospheric conditions of Earth, Mars, and other planets.

1 Introduction

Underexpanded viscous jets have become widely used to study nonequilibrium thermo- and gas-dynamic processes in hypersonic rarefied gas flows [1-4] and aerothermodynamic characteristics of hypersonic vehicle models in wind tunnels [5, 6]. The objective of the present study is to analyze the shapes of underexpanded viscous jets, hypersonic regions inside the jets, diffusive, translational and rotational nonequi-librium processes there, and to apply the jet theory to hypersonic aerodynamic research. Using the method of deformable coordinates, the asymptotic solutions are found for jet parameters in the hypersonic region. Rotational-translational relaxation is analyzed by the numerical solutions of the Navier-Stokes equations in terms of classical and quantum concepts. The aerodynamic characteristics of wedges and plates were studied in rarefied jet flows of helium, argon, nitrogen, and carbonic acid. Similarity parameters and fundamental laws for the aerodynamic characteristics are discussed.

2 Inviscid Gas Jets

Ashkenas and Sherman [1], Muntz [2], Gusev and Klimova [7], Rebrov [8] and others analyzed the structure of inviscid gas jets in detail. They found that the flow inside the jet bounded by shock waves becomes significantly overexpanded relative to the outside pressure p_a. The overexpansion has a maximum value. If sonic Mach number $M_j = 1$ in the initial cross section of the jet, and if the pressure $p_j \gg p_a$, this value is determined by the location of the front shock wave ("Mach disk") on the jet axis r_d [1]:

$$r_d/r_j = 1.34 \, (p_0/p_a)^{½} \qquad (1)$$

The overexpansion phenomenon is very important for aerodynamic experiments in vacuum chambers. In this case the restoration of the pressure occurs automatically, without the use of a diffuser [5-7, 9-10].

The following features of the jet structure were put into consideration during the develop-

ment of approximate analytical and numerical solutions to adequately describe the properties of the flow in various jet areas: a) the bow layer of compressed gas (known as the barrel shock) is detached from the nozzle exit; b) the flow in this detachment area could be approximated by parameters in the Prandtl-Meyer expanding flow 7]; c) at pressure ratio $P = p_0/p_a \gg 1$, the Mach disk exists; its location could be estimated by semi-empirical formula from Eq. (1) that includes the similarity parameter P; d) two areas (separated by the barrel shock and the Mach disk) are independent: internal and external flows that have different characteristics; and e) viscous effects are significant at the nozzle wall, the nozzle exit edge, and near the barrel shock and the Mach disk. At large distances from the nozzle exit the isentropic inviscid flow in a jet asymptotically approaches, along the ray $\varphi =$ const, the flow from a spherical source having an intensity which varies from ray to ray [7, 9].

Following Refs. 9-10, consider the steady expansion of a jet from an axisymmetric nozzle of exit radius r_j. For an inviscid gas flow in a hypersonic region the following asymptotic solution [10] of the Euler equations was found:

$$u'=u_0+u_1\times z^{2(\gamma-1)}+...; \quad z=r_*'(\varphi)/r' \qquad (2)$$

$$v'=v_1\times z^{2(\gamma-1)}\times d/d\varphi[\ln r_*'(\varphi)]+... \qquad (3)$$

$$\rho'=1/u_0\times z^2+... \qquad (4)$$

$$T'=\theta_1\times z^{2(\gamma-1)}+... \qquad (5)$$

$$p'=\theta_1/u_0\times z^{2\gamma}+... \qquad (6)$$

$$u_0=[(\gamma+1)/(\gamma-1)]^{1/2} \qquad (7)$$

$$u_1=-\theta_1/(\gamma^2-1)^{1/2} \qquad (8)$$

$$v_1=-2\theta_1/\{u_0[1-2(\gamma-1)]\} \qquad (9)$$

$$\theta_1=1/(u_0)^{(\gamma-1)} \qquad (10)$$

$$r_*'(\varphi)= r_*(\varphi)/r_j \qquad (11)$$

Here $r_*(\varphi)$ is a function of angle φ, and variables are made dimensionless relative to their critical

values at Mach number $M = 1$. Gusev et al. [7,9] found that at large distances from the nozzle exit the isentropic flow in a jet asymptotically approaches, along each ray $\varphi =$ const, the flow from a spherical source having an intensity which varies from ray to ray. The values of function $r_*(\varphi)$ can be found numerically by the method of characteristics [7].
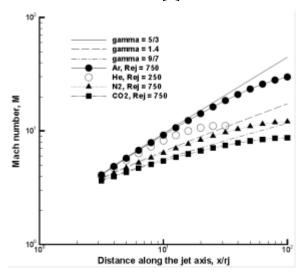

Fig. 1 Mach number M along the axis of axisymmetric jets of argon, helium, nitrogen, and carbonic acid.
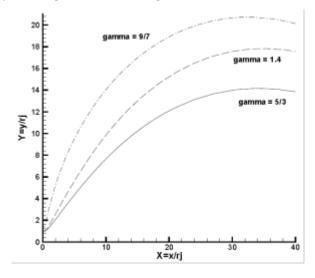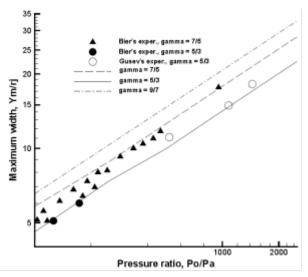

Fig. 2 Barrel shocks of inviscid axisymmetric jets for various gases at pressure ratio $p_0/p_a = 1000$.

Using Eqs. (2-11) we can find the asymptotic solution for Mach number M along the axis of an axisymmetric nonviscous gas jet at large distances $r' \gg 1$:

$$M=(u_0)^{0.5(\gamma+1)}\times[r'/ r_*'(0)]^{(\gamma-1)} \qquad (12)$$

The result of calculations of M is presented in Fig. 1 for monatomic ($\gamma = 5/3$) and diatomic ($\gamma = 1.4$) gases, and carbonic acid ($\gamma = 9/7$).

When the flow within the jet is over-expanded relative to the external pressure p_a, a compression shock with a compression layer adjacent to it develops within the jet. In the case of an axisymmetric jet expanding from a sonic orifice ($M_j = 1$), the method of solving this problem was offered in [7]. Following this technique (with minor corrections), the shock shapes were calculated for gases with different parameters γ and p_0/p_a. The results of calculations for $M_j = 1$, $p_0/p_a = 1000$, and $\gamma = 5/3$, 1.4, and 9/7 are shown in Fig. 2.
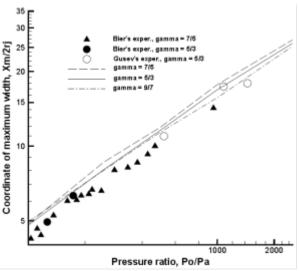

Fig. 3 *Top*: **The maximum width $Y_m = y_m/r_j$ of inviscid axisymmetric jets ($M_j = 1$) for gases with different γ and at various pressure ratios p_0/p_a.** *Bottom*: **The axis coordinate x_m of the width y_m.**

The dimensions (x_m, y_m) of the jet expanded from a nozzle are shown in Fig. 2. They indicate the maximum distance of the compression shock from the jet axis as a function of p_0/p_a. The numerical results (curves) correlate well with the experimental data from [7] ($\gamma = 5/3$, open circles) and [11] ($\gamma = 5/3$, filled circles; $\gamma = 1.4$, triangles).

3 Viscous Gas Jets

The analysis of strongly underexpanded jets of viscous gas was performed by Gusev et al. [5, 9], Riabov [10], and Gusev and Mikhailov [12]. It was shown that at distances $r' = O(Re_j^\omega)$, $\omega = 1/[2\gamma-1-2(\gamma-1)n]$, from the source in the flow, dissipative processes become important and the asymptotic solutions [see Eqs. (2-6)] are not applicable in this region. To find the solution here we use the Navier-Stokes equations in a spherical coordinate system [9] with the origin in the nozzle exit. These new independent and dependent variables should be introduced:

$$W = (u' - u_0)/\zeta^\lambda, \quad \lambda = 2\omega(\gamma-1) \quad (13)$$

$$V = v'/\zeta^\lambda \quad (14)$$

$$\Theta = T'/\zeta^\lambda \quad (15)$$

$$X = r_*'(0)/(r'\zeta^\omega) \quad (16)$$

$$\zeta = 4/[3Re_j r_*'(0)] \quad (17)$$

After the change and the transition to $\zeta \to 0$, we obtain the solution of the Navier-Stokes equations [9, 10] at $n \neq 1$:

$$W = -\Theta/[u_0(\gamma-1)] - u_0\Theta^n/(r_0^2 X) \quad (18)$$

$$\Theta = \{\gamma(\gamma+1)(1-n)\omega/(r_0^2 X) \quad (19)$$
$$+ \theta_1^{1-n}(r_0 X)^{(1-\omega)/\omega}\}^{1/(1-n)}$$

$$r_0^2(\partial V/\partial X - V/X) - (\gamma u_0 X)^{-1}\partial(r_0^2\Theta)/\partial\varphi \quad (20)$$
$$+ nu_0\Theta^{n-1}(2X^2)^{-1}\partial\Theta/\partial\varphi = 0$$

$$r_0 = r_*'(\varphi)/[r_*'(0)] \quad (21)$$

This solution correlates with the solution of Freeman and Kumar [13] at $\varphi = 0$. Therefore, the viscous flow along the axis of an axisymmetric jet at large distances from the

nozzle exit asymptotically approaches the flow from a spherical source. Parameter $r_*'(0)$ can be approximated by functions [7] of M_j and γ.

The influence of viscosity on the gas flow near the jet axis was analyzed by Gusev et al. [9, 12, 14] in terms of the one-dimensional analogy. The influence of dissipative viscous effects on velocity and density along the jet axis is insignificant. The results of calculations of Mach number M along the axis of the axisymmetric jet of a viscous gas are presented in Fig. 1 for Ar ($Re_j = 750$), helium ($Re_j = 250$), nitrogen ($Re_j = 750$), and carbonic acid ($Re_j = 750$) at stagnation temperature $T_s = 295$ K.

The present analysis demonstrates the equivalence of the flow in the hypersonic region of a jet to one-dimensional spherical flow. Therefore, we continue the analysis of kinetic effects in the translational and rotational nonequilibrium flows based on the model of the spherical gas expansion. The binary mixture flows were studied in Refs. 10, 15, and 16.

4 Translational Relaxation of a Spherical Expanding Gas

In the present study, kinetic effects in the spherical expanding flows of argon into vacuum have been studied using the DSMC technique [17] and code [16, 17] (modified for flows with spherical symmetry) at the Knudsen numbers (based on the sonic radius of the spherical source, r_*) from 0.0015 to 0.015.

The inner boundary conditions for velocity u, temperature T, and number density N have matched the transonic continuum solutions [16] at $r/r_* = 1.05$ and selected values of Knudsen number Kn_*.

Code validation was established by using the methodology of Bird [17] and Riabov [16]. The most important parameters of the kinetic approach (mesh size, number of simulating molecules, and time step) have been varied to obtain a reliable solution. The cell geometry has been chosen to minimize the changes in the macroscopic properties (temperature, pressure, and density) across the individual cell [16, 17]. In all cases the criterion [17] for the time step t_m has been realized, $1 \times 10^{-10} \leq t_m \leq 1 \times 10^{-8}$ s. Under

these conditions, gas-dynamic parameters are converged with respect to the time step. The ratio of the mean separation between collision partners to the local mean free path and the ratio of the time step to the local mean collision time has been well under unity over the flowfield.
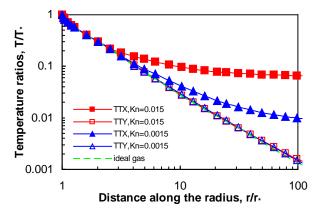

Fig. 4 Parallel (*TTX*) and transverse (*TTY*) temperature distributions in the spherical expansion of argon into vacuum at $Kn_* = 0.015$ and 0.0015.

The DSMC results of the argon expansion from a spherical sonic source into a vacuum (as the outer boundary) are shown in Fig. 4 for two values of the Knudsen number, $Kn_* = 0.015$ (Reynolds number $Re_* = 124$) and 0.0015 ($Re_* = 1240$). The major effect of freezing the parallel temperature TTX can be observed. Bird [17] and Cercignani [18] discussed the "freezing" effect in detail. The point of a gradual rise of the parallel temperature TTX above the continuum value is associated with the breakdown of continuum flow in expansions [17]. The transverse temperature TTY follows the temperature in the isentropic expansion.

5 Rotational Relaxation of a Freely Expanding Gas

Marrone [19] and Borzenko et al. [20] studied the translational-rotational (R-T) relaxation in the expansion of a molecular gas into a vacuum. A significant drop in the gas density downstream leads to a decrease in the number of molecular collisions and, as a result, the departure of the rotational energy E_R from the equilibrium value $E_{R,eq}$ is observed. Lebed and Riabov [21] studied another cause for the rotational energy departure, which could be

explained in terms of quantum concepts. Because of the significant decrease in kinetic temperature T_t, the Messy adiabatic parameter [22], describing energy transfer between highly excited rotational levels unable to relax, becomes larger than unity. Adiabatic collision conditions are realized at a certain temperature, which is a characteristic for each rotational level. At these conditions, the rotational transfer probability begins to decrease significantly [21], and the relaxation time τ_R increases.

Using the technique of Lebed and Riabov [21], the rotational-translational relaxation times were calculated for nitrogen (see Fig. 5) at conditions of aerodynamic experiments in underexpanded jets.
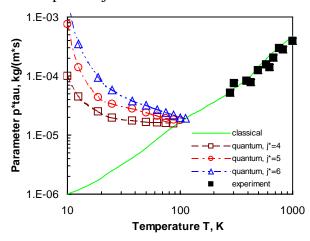

Fig. 5 Relaxation time τ_R of molecular nitrogen vs. kinetic temperature T_t: solid line - Parker's model [23]; open symbols - quantum rotational levels $j^* = 4$, 5, and 6 [21]. Experimental data from Refs. 24-25.

The relaxation times calculated by Parker [23] are shown in Fig. 5 as solid line. This data could be approximated by the function [10]:

$$p\tau_R = CT_t^m \qquad (22)$$

with the parameters $m = 1$ and $C = 1.65 \cdot 10^{-7}$ kg/m·sec·K. The calculations based on the classical concept do not show a tendency of increasing $p\tau_R$ with the decrease of T_t under adiabatic rotational energy exchange conditions. At temperatures $T_t > 273$ K, numerical results correlate well with experimental data [24, 25].

In the expansion of nitrogen, starting at a stagnation temperature $T_s = 300$ K, the maximum population of molecules occurs at

rotational levels j^* from 6 to 4. Following Refs. [21, 22], the result of calculating $p\tau_R$ for $j^* = 6$, 5, and 4 is shown in Fig. 5 (empty triangles, circles, and squares, correspondingly). These values of $p\tau_R$ increase with decrease of T_t. At $T_t > 100$ K, the adiabatic condition breaks down, and the parameter $p\tau_R$ could be calculated by the Parker's model [23].

For qualitative estimations, it is possible to replace the energy relaxation time by the relaxation time of the level j^*. This approximation method correctly represents the nature of the R-T nonequilibrium process, i.e., an increase of $p\tau_R$ with decreasing T_t.
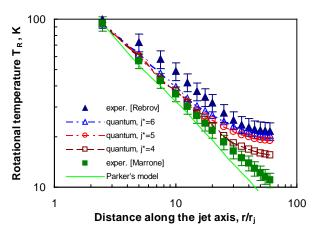

Fig. 6 Rotational temperature T_R along the axis of nitrogen jet. Experimental data from Refs. 19-20.

Figure 6 shows the distributions of rotational temperature T_R along the axis of nitrogen jet. The result of using the classical mechanics concept [23] is shown there by the solid line. The curves marked by empty triangles, circles, and squares were obtained in terms of the quantum concept [21] for values of $p\tau_R$ at $j^* = 6$, 5, and 4, correspondingly. In the calculation it was assumed that the main R-T relaxation parameter was $K_* = \rho_* u_* r_*/(p\tau_R)_* = 2730$, $p_s r_j = 240$ torr·mm and $T_s = 290$ K.

The experimental results for T_R along the axis of a nitrogen jet were obtained by Marrone [19] (filled squares), and Borzenko et al. [20] (triangles). The experimental data are upper and lower bounds on the distribution of rotational energy along the flow. Numerical results, based on the quantum concept of rotational energy exchange, correlate well with the experimental

data [20]. The data contradicts the classical model predictions [23] of T_R.

The experimental and computational results demonstrate the necessity of a consideration of the quantum concept in describing R-T relaxation in underexpanded jets. This concept was used by Gochberg and Haas [26] in evaluating rotational relaxation models in expanding flows of nitrogen under different low-density conditions.

6 Rotational Relaxation in Viscous Gas Flows

The combined effect of the rotational-translational relaxation and dissipative processes of viscosity and conductivity in expanding flows was analyzed by Riabov [27, 28], Lebed and Riabov [29], Skovorodko [30], and Rebrov and Chekmarev [31]. The system of the Navier-Stokes equations and the relaxation equation, based on the τ - approximation [28, 29], has been solved by the implicit numerical technique [27]. Solutions of the boundary value problem depend on the following parameters: Reynolds number Re_*, pressure ratio $P = p_*/p_a$, T_{sa}, n, m, and K_*. The computational results confirmed the delay [30, 31] of the rotational temperature compared to the translational one. The decrease rate for T_R slows down with the gas expanding in the inner supersonic area of the flow that leads to its "frozen" value. Rotational-translational equilibrium never exists near the shock wave in such flow, and $T_R > T_t$.
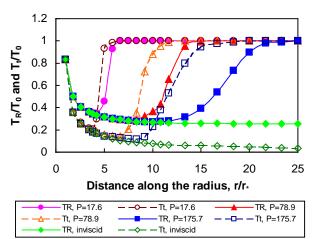

Fig. 7 Rotational T_R and translational T_t temperatures in spherical flow at different pressure ratios P.

As the result of gas compression in the shock wave, rapid increase of rotational temperature occurs. Following the point $T_R = T_t$ the values of translational temperature begin to increase too. As the gas expands in the subsonic area of the flow behind the shock wave, gradually temperature reaches the value of T_{sa}.

The distributions of T_R and T_t are shown in Fig. 7 at different pressure ratios p_*/p_a under the conditions: $Re_* = 161.83$; $K_* = 28.4$; $Pr = n = 0.75$; $T_{sa} = 1.2T_*$. Inviscid flow parameters T_R and T_t (diamonds) are obtained by the method of Lebed and Riabov [21]. Viscosity and thermal conductivity have a minor influence on the distribution of rotational temperatures in the inner supersonic region of the flow [27].

The numerical analysis [10,21,28] showed that the main parameters, which influence the relaxation process, are K_* and the approximation function $p\tau_R(T_t)$. The decrease of the relaxation parameter K_* leads to a higher "frozen" value of rotational temperature [10, 28, 30].

The effect of "frozen" rotational energy can be significant for the prediction of heat transfer to the surface of the model [27], for estimation of the perturbation zone near the model [28], as well as for correct displacement of the model in the supersonic region of the jet [10, 27].

7 Similarity Criteria for Aerodynamic Experiments in Underexpanded Jets

The Reynolds number Re_0, in which the viscosity coefficient was calculated by means of stagnation temperature T_s, can be considered as the main similarity parameter for modeling hypersonic flows in continuum, transitional and free-molecular flow regimes [5]. Using this criterion and other similarity parameters (γ, M_∞), it is possible to perform other well-known parameters, such as the interaction parameter χ for pressure approximation and the viscous-interaction parameter V for skin-friction approximation [1-4]:

$$\chi = M_\infty^2/[0.5(\gamma-1)Re_0)]^{0.5} \qquad (23)$$

$$V = 1/[0.5(\gamma-1)Re_0)]^{0.5} \qquad (24)$$

The Reynolds number Re_0 also scales the flow rarefaction, which is characterized by the Knudsen number $Kn_{\infty,L}$ [5, 17], as well as by the viscous-interaction parameter V [1-4].

The similarity criteria for hypersonic flows in the transitional regime, which is between continuum media and free molecular flow, were defined by Gusev et al. [5-6]. These studies offered the method of strongly underexpanded jets for aerodynamic experiments in order to receive experimental data in the broad range of changes of the main similarity criterion Re_0. The value of Re_0 can be easily changed by relocation of a model along the jet axis at different distances x from a nozzle exit ($Re_0 \sim x^{-2}$). The presence of a non-uniform field in the expanding flow and experimental errors (5-8%) were evaluated by techniques described in [6, 10, 32]. Using this method, fundamental laws of hypersonic streamlining of bodies were discovered and numerous experimental data on aerodynamic and thermal characteristics of different bodies was received [5, 6, 33, 34].

In the present study, the role of other similarity parameters was studied: Mach number M_∞, temperature factor t_w; specific heat ratio γ; and parameter n in the viscosity coefficient approximation $\mu \sim T^n$. The results obtained permit the evaluation of the influence of these similarity criteria on the aerodynamic characteristics of the bodies of simple shapes in the transitional flow regime. The testing was performed in underexpanded viscous jets in a vacuum wind tunnel [6,10] at $T_s = 295$ K and $T_s = 950$ K with gases: He, Ar, N_2, and CO_2. The axisymmetric sonic nozzles ($M_j = 1$) with different radii of the critical cross-sections r_j were used for obtaining the hypersonic flow. Plates and wedges were selected as working models. The coordinate of the Mach disk r_d was determined from Eq. (1). The influence of viscous and nonequilibrium effects on the density and the flow velocity for all the gases was insignificant. Therefore, the criterion Re_0 and dynamic pressure were calculated using the inviscid flow parameters obtained by the method of characteristics in the processing of the testing data. The errors of experimental data (6-10%) were estimated in [5, 10, 33, 34].

8 The Results of Testing

8.1 Influence of Mach Number M_∞

The flow near the body strives for the certain limited condition at the continuous increase of Mach number M. This condition can be reached for some bodies at moderate values of M_∞ [35]. Numerous exact solutions and testing data [6] on streamlining of such bodies, which were obtained at large values of Reynolds number, confirm this conclusion. The hypersonic stabilization regime remains the same for the transitional flow conditions [10, 36] at $K = M_\infty\theta \gg 1$ in the case of streamlining of the thin bodies when the angle θ between the generatrix of the body surface and the direction of the upstream flow becomes small enough. This regime is realized at smaller values of M_∞, if the angle θ increases.
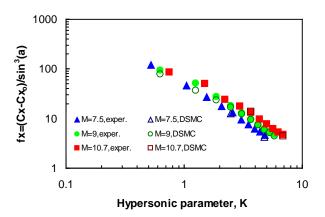

Fig. 8 Modified drag coefficient vs. hypersonic parameter K for the blunt plate ($\delta = 0.06$).
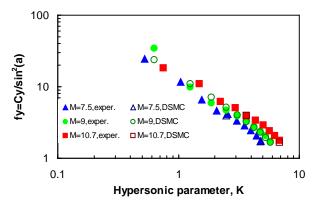

Fig. 9 Modified lift coefficient vs. hypersonic parameter K for the blunt plate ($\delta = 0.06$).

The results of such studies were obtained for the plate having relative thickness $\delta = h/l = 0.06$ at the angle of attack α. The testing was conducted in helium ($\gamma = 5/3$) at $Re_0 = 2.46$, and temperature factor $t_w = 1$ (the wall temperature was $T_w = 295$ K in all experiments). The selection of helium as the working gas is explained by the constant value of exponent $n = 0.64$ within the range of temperature changes.

The experimental data for aerodynamic coefficients c_x and c_y for the plate at the angle of attack α are shown in Figs. 8 and 9. The results for the values of the Mach number $M_\infty = 7.5$ (filled triangles), 9 (circles), and 10.7 (squares) are presented in terms of the functions [35] $f_x = (c_x - c_{x0})/\sin^3\alpha$ and $f_y = c_y/\sin^2\alpha$, and the parameter $K = M_\infty\sin\alpha$. The model length and the planform area were selected for the calculation of the aerodynamic parameters c_x, c_y, and Re_0. The comparison of the testing data with the calculated ones, obtained by the direct simulation Monte-Carlo (DSMC) technique [36] is shown in the same figures.

The correlation of the results for the functions [35] f_y and f_x is well acceptable. At different magnitudes of the Mach number M_∞, the values of the functions are almost the same at $K \geq 3$ or at $\alpha \geq 24$ deg. This study indicates that the principle of independence of the hypersonic flow of the Mach number can be applied at the smaller values of M_∞ for the blunt bodies, not for the thin bodies at small angles α.

The dependency of the drag and lift coefficients c_x and c_y of the wedge ($2\theta = 40$ deg) on the angle of attack was obtained by testing in the helium flow at $Re_0 = 4$, $t_w = 1$, $M_\infty = 9.9$ (filled circles), and $M_\infty = 11.8$ (squares) (see Figs. 10 and 11). The base area of the wedge and its length were taken as the surface and linear measures. The comparison of the testing data with the data calculated by the direct simulation Monte-Carlo (DSMC) technique [36] is shown in the same figures. The obtained results indicate the weak dependency of aerodynamic coefficients on the Mach number M_∞ in this regime. This is also proved by the calculated data of the free molecular flow [37] (solid line) shown in Figs. 10-11. The lift in the

transitional regime is bigger than the lift for the free molecular flow by a factor of 1.25.
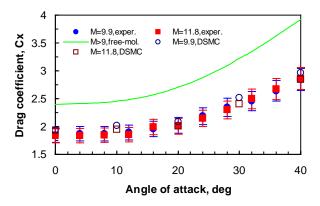

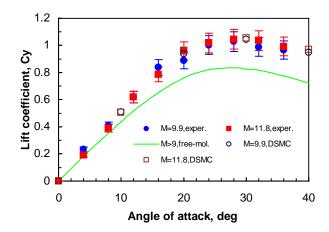**Fig. 10 Drag coefficient c_x of the wedge ($2\theta = 40$ deg) at $Re_0 = 4$ and various Mach numbers M_∞.**

Fig. 11 Lift coefficient c_y of the wedge ($2\theta = 40$ deg) at $Re_0 = 4$ and various Mach numbers M_∞.

The conducted research confirms the hypersonic stabilization (*M*-independence) principle in the transitional regime [6].

8.2 The influence of the specific heat ratio γ

In the free-molecular flow regime [37], the aerodynamic characteristics of bodies depend on the normal component of the momentum of the reflected molecules, which is a function of γ. The same phenomenon [6, 36] was observed at the transitional conditions. The drag coefficient of the thin bodies will be proportionate to ($\gamma + 1$) at the regime of hypersonic stabilization [6]. The identical conclusion is derived from the testing studies conducted with argon ($\gamma = 5/3$), nitrogen ($\gamma = 1.4$), and carbonic acid ($\gamma = 9/7$). The dependencies of the drag coefficient c_x of

the wedge (2θ= 40 deg) for Ar (filled circles), N_2 (squares), and CO_2 (triangles) are shown in Fig. 12 at various Reynolds numbers Re_0. Here testing data are compared with the data calculated by the DSMC technique [36].
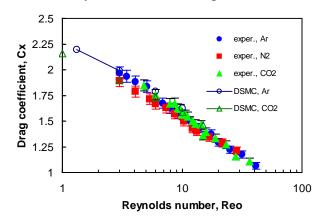

Fig. 12 Drag coefficient c_x of the wedge (2θ = 40 deg) for various gases vs. the Reynolds number Re_0.

The influence of specific heat ratio on the drag coefficient is more significant for small values of the Reynolds number $Re_0 < 10$. In the free molecular regime ($Re_0 \to 0$) [6, 37] a small increase of the drag coefficient c_x is observed as the specific heat ratio γ grows. This increase is caused by the impulse of the reflected molecules at $t_w = 1$. The degree of this influence was evaluated by Gusev et al. [6] as 3%. Identical dependency was found in the testing for transitional regime at $Re_0 < 10$ (5%). As the number Re_0 increases, this influence decreases.
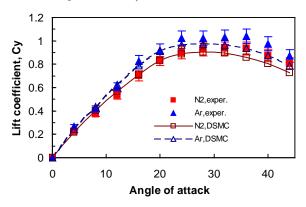

Fig. 13 Lift coefficient c_y of the wedge (2θ = 40 deg) at Re_0 = 3 and various gases.

This phenomenon takes place in the case of streamlining of the wedge (2θ = 40 deg) at $0 < \alpha < 40$ deg and $Re_0 = 3$. The experimental data for

Ar and N_2 and results calculated by the DSMC technique [36] are shown in Fig. 13. The correlation of the data demonstrates a significant difference (10%) in the values of c_y.
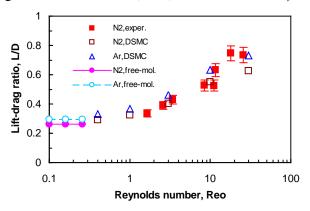

Fig. 14 Lift-drag ratio of the blunt plate (δ = 0.1) at α = 20 deg in Ar and N_2 vs. Reynolds number Re_0.
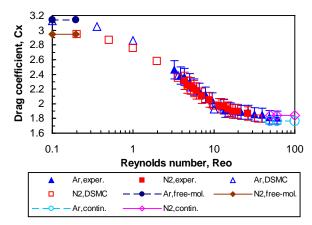

Fig. 15 Drag coefficient c_x of the plate at α = 90 deg for argon and nitrogen vs. the Reynolds number Re_0.

This effect is estimated as 4% for the lift-drag ratio of the blunt plate at α = 20 deg and various Reynolds numbers (see Fig. 14).

The dependencies of C_x of the disc for Ar (filled triangles) and N_2 (filled squares) are shown in Fig. 15 for a wide range of Reynolds number, Re_0. At the same parameters of the upstream flow, numerical data obtained by the DSMC technique [36] for Ar and N_2 are compared with experimental data.

8.3 The influence of the viscosity parameter n

The helium-argon pair is acceptable for testing to analyze the influence of viscosity parameter

n, which is closely related to the exponent *s* in the exponential law [37] of molecular interactions, and $n = \frac{1}{2} + 2/(s - 1)$. The parameter *n* for argon and helium has approximately constant values and differ significantly ($n_{Ar} > n_{He}$) at $T < 300$ K [10].
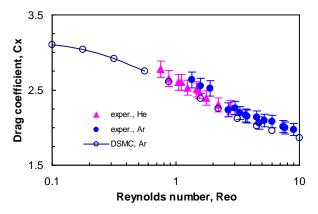

Fig. 16 Drag coefficient c_x of the plate at $\alpha = 90$ deg in helium and argon vs. the Reynolds number Re_0.

The testing of the plate at $\alpha = 90$ deg (see Fig. 16) was conducted in He (triangles) and Ar (circles) at $t_w = 1$, $T_s = 295$ K. The experimental data indicates that the insignificant increase (about 5%) of the drag coefficient c_x occurs with the increase of the exponent *n* at $Re_0 \leq 2$. The experimental data correlates well with the results calculated by the DSMC technique [36].

The experimental and computational results for disks, wedges and plates [6, 36] indicate the insignificant influence (about 5%) of viscosity parameters *n* on aerodynamic characteristics of the bodies in the transitional hypersonic stabilization regime.

8.4 The influence of the temperature factor t_w

Compared to other similarity parameters, the temperature factor ($t_w = T_w/T_0$) is the most important [5-7, 9]. As an example, experimental data for lift-drag ratio of a plate ($\delta = 0.1$) is shown in Fig. 17 for wide range of Reynolds numbers. The ratio changes non-monotonically from the continuum to the free-molecular flow regime. Maximum values occur in the transitional flow regime. The influence of the temperature factor can be estimated as 35% for the lift-drag ratio. The DSMC numerical results [36] correlate well with the experimental data.

Decreasing the temperature factor significantly decreases the pressure at the body surface in comparison with the tangential stresses [6, 10]. Therefore, the lift coefficient is the most sensitive aerodynamic parameter to changes of t_w in the transitional flow regime (see Fig. 17).
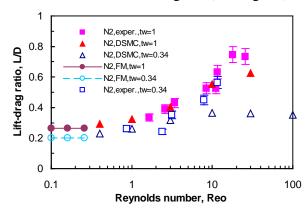

Fig. 17 Lift-drag ratio for the blunt plate ($\delta = 0.1$) vs. Reynolds number Re_0 in nitrogen at $\alpha = 20$ deg and various temperature factors.

Concluding Remarks

The methods used in this study allow the user to study effectively the hypersonic viscous flows of the monatomic and polyatomic gases in the underexpanded jets, and flows near probes in the transitional regime between free-molecular and continuum regimes. Good correlation is noticed between testing data and calculated results obtained by the direct simulation Monte-Carlo technique. The acquired information about hypersonic rarefied gas flows in underexpanded jets could be effectively used for investigation and prediction of the aerodynamic characteristics of hypersonic vehicle flights in complex atmospheric conditions of the Earth, Mars and other planets.

Acknowledgments

References

[1] Ashkenas H and Sherman F. The structure and utilization of supersonic free jets testing in low-density wind tunnels. *Proc. 4th Intern. Symposium on RGD*, Toronto, Canada, Vol. 2, pp. 84-105, 1965.

[2] Muntz E. Rarefied gas dynamics. *Annual Review of Fluid Mechanics*, Vol. 21, pp. 387-417, 1989.

[3] Lengrand J, Allegre J and Raffin M. Experimental investigations of underexpanded thruster plumes. *AIAA Journal*, Vol. 14, No. 5, pp. 692-694, 1976.

[4] Boyd I, Penko P, Meissner D and DeWitt K. Experimental and numerical investigations of low-density nozzle and plume flows of nitrogen. *AIAA Journal*, Vol. 30, No. 10, pp. 2453-2461, 1992.

[5] Gusev V, Kogan M and Perepukhov V. The similarity and aerodynamic measurements in hypersonic transitional regime. *Uchenyye Zapiski TsAGI*, Vol. 1, No. 1, pp. 24-31, 1970 (in Russian).

[6] Gusev V, Erofeev A, Klimova T, Perepukhov V, Riabov V and Tolstykh A. Theoretical and experimental investigations of flow over simple shape bodies by a hypersonic stream of rarefied gas. *Trudy TsAGI*, No. 1855, pp. 3-43, 1977 (in Russian).

[7] Gusev V and Klimova T. Flow in underexpanded jets. *Fluid Dynamics*, Vol.3, No.4, pp.121-125, 1968.

[8] Rebrov A. Free Jets in Vacuum Technologies. *Journal of Vacuum Science and Technol*ogy, *Ser. A*, Vol. 19, No. 4, pp. 1679-1687, 2001.

[9] Gusev V, Klimova T and Riabov V. Similarity of flows in strongly underexpanded jets of viscous gas. *Fluid Dynamics*, Vol. 13, No. 6, pp. 886-893, 1978.

[10] Riabov V. Aerodynamic applications of underexpanded hypersonic viscous jets. *Journal of Aircraft*, Vol. 32, No. 3, pp. 471-479, 1995.

[11] Bier K and Schmidt B. Zur Form der Verdichtungsstöße in frei expandierenden Gasstrahlen. Zeitschrift für angewandte Physik, Bd. 13, n. 11, S. 494-500, 1961.

[12] Gusev V and Mikhailov V. Similarity of flows with expanding jets. *Uchenyye Zapiski TsAGI*, Vol. 1, No. 4, pp. 22-25, 1970 (in Russian).

[13] Freeman N and Kumar S. On the solution of the Navier-Stokes equations for a spherically symmetric expanding flow. *Journal of Fluid Mechanics*, Vol. 56, Part 3, pp. 523-532, 1972.

[14] Gusev V and Zhbakova A. The flow of a viscous heat-conducting compressible fluid into a constant pressure medium. *Proc. 6th Intern. Symp. on RGD*, Cambridge, MA, USA, Vol. 1, pp. 847-862, 1969.

[15] Gusev V. and Riabov V. Spherical expansion of a binary gas mixture into a flooded space. *Fluid Dynamics*, Vol. 13, No. 2, pp. 249 - 256, 1978.

[16] Riabov V. Kinetic phenomena in spherical expanding flows of binary gas mixtures. *Journal of Thermophysics and Heat Transfer*, Vol. 17, No. 4, pp. 526-533, 2003.

[17] Bird G. *Molecular gas dynamics and the direct simulation of gas flows.* 1st edition, Oxford University Press, 1994.

[18] Cercignani C. *Rarefied gas dynamics: from basic concepts to actual calculations*. Cambridge University Press, Cambridge, England, UK, 2000.

[19] Marrone P. Temperature and density measurements in free jets and shock waves. *Physics of Fluids*, Vol. 10, No. 3, pp. 521-538, 1967.

[20] Borzenko B, Karelov N, Rebrov A and Sharafutdinov R. Experimental investigation of the molecular rotational level population in a free jet of nitrogen. *Journal of Applied Mechanics and Technical Physics*, Vol. 17, No. 5, pp. 20-31, 1976.

[21] Lebed I and Riabov V. Quantum effects in rotational relaxation of a freely expanding gas. *Journal of Applied Mechanics and Technical Physics*, Vol. 20, No. 1, pp.1-3, 1979.

[22] Lebed I and Umanskii S. Rotational relaxation of strongly excited molecules. *High Energy Chemistry*, Vol. 10, No. 6, pp. 501-506, 1976 (in Russian).

[23] Parker J. Rotational and vibrational relaxation in diatomic gases. *Physics of Fluids*, Vol. 2, No. 4, pp. 449-462, 1959.

[24] Brau C and Jonkman R. Classical theory of rotational relaxation in diatomic gases. *Journal of Chemical Physics*, Vol. 52, No. 2, pp. 474-484, 1970.

[25] Lordi J and Mates R. Rotational relaxation in nonpolar diatomic gases. *Physics of Fluids*, Vol. 13, No. 2, pp. 291-308, 1970.

[26] Gochberg L and Haas B. Evaluation of rotational relaxation rate models in low-density expanding flows of nitrogen. AIAA Paper 95-2070, 1995.

[27] Riabov V. Rotational relaxation in spherically expanding flow of viscous gas. *Uchenyye Zapiski TsAGI*, Vol. 9, No. 5, pp. 58-64, 1978 (in Russian).

[28] Riabov V. Gas dynamic equations, transport coefficients, and effects in nonequilibrium diatomic gas flows. *Journal of Thermophysics and Heat Transfer*, Vol. 14, No. 3, pp. 404-411, 2000.

[29] Lebed I and Riabov V. Rotational relaxation time and transfer coefficients in a diatomic gas. *Journal of Applied Mechanics and Technical Physics*, Vol. 24, No. 4, pp. 447-454, 1983.

[30] Skovorodko P. Rotational relaxation in a gas expanding into vacuum. *Rarefied Gas Dynamics*, Inst. Teplofiz. Sib. Otd. Akad. Nauk SSSR, Novosibirsk, Russia, pp. 91-112, 1976 (in Russian).

[31] Rebrov A and Chekmarev S. Spherical expansion of rotational relaxing viscous gas into flooded space. *Rarefied Gas Dynamics*, Inst. Teplofiz. Sib. Otd. Akad. Nauk SSSR, Novosibirsk, Russia, pp. 113-119, 1976 (in Russian).

[32] Nikolaev V. Aerodynamic and thermal characteristics of simple shape bodies in a nonuniform flow. *Trudy TsAGI,* No. 1709, pp. 3-25, 1975 (in Russian).

[33] Gusev V, Klimova T and Lipin A. Aerodynamic characteristics of the bodies in the transitional regime of hypersonic flows. *Trudy TsAGI*, Issue 1411, pp. 3-53, 1972 (in Russian).

[34] Gusev V, Nikol'skii Yu and Chernikova L. Heat transfer and hypersonic rarefied gas flow streamlining of the bodies. *Heat and Mass Transfer*, Minsk, Vol. 1, pp. 254-262, 1972 (in Russian).

[35] Anderson J. *Hypersonic and high temperature gas dynamics*, McGraw-Hill, New York, 1989.

[36] Riabov V. Comparative similarity analysis of hypersonic rarefied gas flows near simple-shape bodies. *Journal of Spacecraft and Rockets*, Vol. 35, No. 4, pp. 424-433, 1998.

[37] Kogan M. *Rarefied gas dynamics*, Academic Press, New York, 1969.

Contact Author Email Address

The contact author email address:
vriabov@rivier.edu

Copyright Statement